OPTIMISATION AND KINETIC STUDIES ON SILVER LEACHING FROM WASTE PRINTED CIRCUIT BOARDS IN SELECTED GREEN SOLVENTS

Abubakar Osafo Kantanka, Benetta Koomson, Emmanuel Mensah Azogba

Department of Materials Engineering, Kwame Nkrumah University of Science and Technology, Kumasi, Ghana;
E-mail: mateng@gmail.com
Corresponding author: abubakarosafo11@gmail.com

ABSTRACT. Organic acids are being explored as biodegradable lixiviants for extracting valuable metals from various sources with a lower environmental footprint. However, studies on using organic acids for silver extraction from waste printed circuit boards (WPCBs) remain limited, particularly regarding process parameters and leaching kinetics. This study employed response surface methodology (RSM) with central composite design (CCD) to optimise acetic and citric acids for silver leaching from WPCBs. Key parameters included are temperature, lixiviant concentration, and leaching time. Kinetic behaviour was analysed using Arrhenius and shrinkage core models. RSM-CCD analyses indicated that the quadratic model effectively predicted silver leaching percentages across the tested factors, with significant effects noted for most parameters, except temperature in the acetic acid system. Optimal silver recovery was 11.48% for acetic acid (38.8°C, 2.5 M, 4 h) and 15.2% for citric acid (37.7°C, 1 M, 1.5 h). Kinetic studies showed leaching was diffusion-controlled, with activation energies of 13.13 kJ/mol for acetic acid and 3.3 kJ/mol for citric acid. Overall, this study sets the foundation for a scalable and environmentally sustainable silver recovery from WPCB.

Key words: silver leaching, citric acid, acetic acid, response surface methodology, kinetic studies

Introduction

For over 6000 years, silver has been and continues to be integral to various aspects of human life (Syed, 2016). While historically valued for its use in jewellery, coins, and silverware, silver now finds extensive use in modern technologies, including electronics and renewable energy, where its superior electrical conductivity and photosensitivity properties are indispensable (Mishra et al., 2021; Click et al., 2024). Silver is primarily recovered as by-product from processing polymetallic sulphide ores of gold, lead, zinc, and copper (Zhang et al., 2024). However, the rising demand for silver in modern applications has led to over-reliance and depletion of these sources. In 2021, silver production met only 48 % out of the total physical demand for silver of ~1 trillion ounces, leaving a sizable deficit. Moreover, this demand was projected to increase by 9.3 % yearly (Cremona and Mestl, 2023). Consequently, the Sustainable Development Goal (SDG) 12, which aims at responsible consumption and production, demands that secondary sources of silver be exploited.

A secondary source of silver that has increasingly garnered the attention of researchers over recent years is the waste of electrical and electronic equipment (WEEE), primarily due to two observations. On one hand, with over 53.6 million tons generated in 2019 and projected to reach 74.7 million tons by 2030, WEEE is becoming one of the fastest-growing solid waste streams in the world. Out of the total amount of WEEE waste generated, only 17.6% has been documented to undergo proper collection, processing, and recycling, while the difference remains unaccounted for (Arshadi and Mousavi, 2014; de Souza et al., 2018; Forti et al., 2020). This creates an ever-growing concern as this waste contains hazardous elements and compounds such as cadmium, lead, mercury, and fluorinated flame retardants, which pose enormous health and environmental hazards, particularly when treated or processed inadequately. On the other hand, waste printed circuit board (WPCB), an integral component of WEEE, contains about 30-40 wt% of valuable metals, including gold, copper, zinc, tin, nickel, and up to about 0.13 wt% silver, amongst others, which is higher than that found in primary sources (Cayumil et al., 2016; Mishra et al., 2021). Thus, ever-increasing volumes of WPCBs will provide an avenue as a secondary source for silver extraction, serving a dual benefit for the metal supply chain and managing the environmental pollution associated with the WPCB accumulation.

Hydrometallurgical recycling has become a widely adopted approach for recovering valuable metals from WPCB owing to its comparatively simple applicability and high extraction efficiency (Marinato et al., 2023; Nan et al., 2024). This approach is a two-stage process consisting of selective metal dissolution (leaching) and purification (ion exchange, precipitation, etc.). Current hydrometallurgical systems have been based on the leaching stage, mostly using cyanide, thiourea, thiosulphate, and inorganic acids such as HCl and HNO_3, amongst others, as lixiviants (Kumari and Samadder, 2022). Unsurprisingly, these lixiviants lead to distinct metal recovery rates, environmental footprints, and other inherent issues. For example, HCl and HNO_3 exhibit higher metal leaching efficiency but at the same time generate chemical-heavy liquid wastes and release gases such as Cl_2 and NO_x, posing a huge threat to the environment. Similarly, the high toxicity of cyanide is a major issue and has resulted in significant efforts for its substitution despite being efficient as a lixiviant. Thiourea and thiosulphate have shown great potential as green alternatives, but are still developing hydrometallurgical processes (Hsu et al., 2019). It, therefore, remains of great interest to find more environmentally sustainable leaching systems for future applications.

Potential environmentally sustainable leaching systems use organic acids as lixiviants (Lisińska et al., 2022). Organic acids are environmentally friendly as they are biodegradable in aerobic and anaerobic conditions, making the liquid waste generated from the leaching process easy to treat. Moreover, they have demonstrated high metal recovery rates from different

sources under varying process conditions, particularly when used in the presence of oxidants. For instance, Li et al., (2013) studied the efficiency of citric, malic, and aspartic acids in leaching lithium and cobalt from spent lithium-ion batteries in the presence of H_2O_2. The results showed that citric and malic acids recovered 100% lithium and 90% cobalt, whereas aspartic acid recovered significantly less. Similarly, (Jadhav et al., 2016a) utilized citric acid in combination with H_2O_2 to leach different metals from large WPCB under varying conditions - citric acid (0.5-2 M) and H_2O_2 concentration (1.5-7.28%), temperature (30-60°C), and stirring speed (0 and 150 rpm). The results showed that under static conditions, a 0.5 M citric acid solution and 5.83% H_2O_2 solution achieved complete dissolution (100%) of Au, Ag, and other base metals within 4 hours at 30 °C. Aydoğan et al. (2024) also studied the dissolution kinetics of metallic Ag in acetic acid by applying the shrinkage core models, revealing a surface-chemical controlled process.

Despite achieving high leaching rates and offering a promising environmentally sustainable option, very few studies have been conducted on using organic acids for leaching silver from WPCB (Birloaga and Vegliò, 2016; Zan et al., 2024). Moreover, the interaction effects of the studied leaching process parameters (temperature, organic acid concentration, time, stirring speed, solid-to-liquid ratio) were not accounted for, as these studies employed the conventional "one factor at a time" experimental approach (Saidan et al., 2012). Furthermore, there is no information on the underlying kinetic mechanism, which is imperative for the scalability of recycling WPCB in organic acid systems.

The present work capitalized on central composite design (CCD) and response surface methodology (RSM) experimental design framework to study silver leaching from WPCB in selected green solvents, namely acetic and citric acids. Unlike the conventional approach, this experimental design framework considers the synergistic effects of selected process parameters: temperature, lixiviant concentration, and leaching time on the leaching systems. These parameters were further optimised to achieve an optimum percentage of silver-leached values. Finally, the dissolution kinetic mechanisms were also investigated using the Arrhenius and shrinkage core (SCMs) models. This research promotes responsible consumption and production (SDG 12), fostering innovation in material recovery (SDG 9), and supporting climate action (SDG 13) through eco-friendly recycling methods that reduce electronic waste and minimise environmental impact.

Materials and Methods

WPCB sample acquisition and preparation

A total mass of 3 kg of WPCB samples from discarded Toshiba laptops (2016 to 2018 models) was collected from the Agbogbloshie area in the southwest of Accra, Ghana. Large components that could not be easily crushed with the available equipment were manually removed from the WPCB samples, after which the samples were hand-broken into smaller pieces. To liberate the metals from non-metallic components and increase the exposed surface area for the leaching, the WPCB samples were crushed and ground into particle sizes smaller than 150 µm with metallic mortar and pestle. The samples were then divided into smaller representative samples of the required mass using the sampling by quartering method for the leaching experiment.

Design of leaching experiments using CCD-RSM

The leaching experiments were designed using the RSM-CCD experimental design framework with Design-Expert Software Version 13. Two levels of three leaching factors: temperature, lixiviant concentration and leaching time, were utilised in the CCD as shown in Table 1. Equation (1) was used to generate a specific number of experimental runs that were used to collect data at specific points. These points included factorial points (to study the main effects and interactions), central points (to estimate pure error or variability), and axial points (to capture curvature effects) (Behera et al., 2018).

$$N = 2^n + 2n + n_c \quad (1),$$

where N is the number of experimental runs, n is the number of factors, 2^n is the number of factorial points, $2n$ is the number of axial points, and $n_c = 6$ is the number of centre points.

Table 1. *The leaching factors and their corresponding range of levels for the RSM-CCD experimental design*

Variable	Name of factor	Range of levels	
		Low	High
A	Temperature (°C)	25	75
B	Lixiviant concentration (M)	1	3
C	Leaching time (h)	1.5	4

Leaching procedure

Acetic and citric acid followed the same leaching protocol, as shown in Fig. 1. The leaching experiments were carried out in an open 1000 mL flat-bottom flask containing a stirring bead, placed on a dual hotplate and magnetic stirrer apparatus equipped with feedback control systems. 100 mL of the required concentration of lixiviant was added to the flat-bottom flask and heated to the predetermined temperatures and times at a constant stirring speed of 250 rpm before introducing 1 g of the representative WPCB sample. The amount of lixiviant used was based on a constant solid-to-liquid ratio of 10 g/L, whereas the concentrations were per the range given by the experimental design, as shown in Table 1. After each leaching test, the mixture was allowed to cool to room temperature, followed by filtration to remove any leach residue, and the leachate was analysed for the silver concentration.

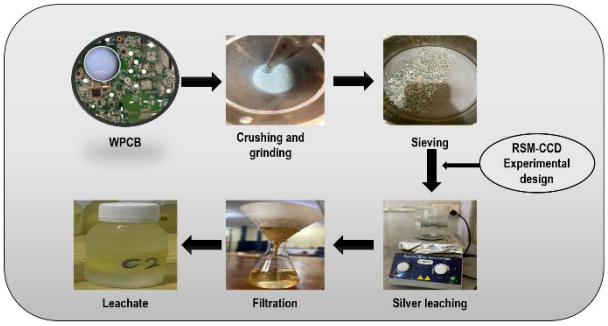


Fig. 1. Schematic representation of the initial WPCB preparation and leaching experimental procedure

Prior to leaching with the organic acids, the leachability of silver from the representative WPCB sample was investigated by performing a leaching test using 40 mL of aqua regia solution at 100 °C and 250 rpm for 1.5 hours. 25 mL of the aqua regia leachate was analysed for silver concentration and was used as the reference point for the estimation of the percentage of silver leached from WPCB (S) in the acetic and citric acids as expressed by equation (2).

$$S = \frac{C_g V_g}{CV} \times 100 \quad (2),$$

where C_g is the concentration of silver in the green leachate (mg/L), V_g is the volume of the green leachate (mL), C is the concentration of silver in the aqua regia leachate (mg/L), and V is the volume of the aqua regia leachate (mL) (de Souza et al., 2018; Han et al., 2020).

Materials characterisation

Chemical compositional analysis of the representative WPCB sample and silver chloride precipitate was performed using a Rigaku NEX CG X-ray fluorescence spectrometer. A Thermofisher Scientific iCAP 7400 Duo ICP-OES spectrometer equipped with a Teledyne ASX-560 autosampler was utilised to determine the concentration of silver in aqua regia and organic acid leachates. To investigate the mineralogical composition of the WPCB, a representative sample was analysed with a Cu-kα source (λ= 1.5406 nm) Bruker D2 Phaser 2nd Gen X-Ray diffractometer operating at 30 kV and 10 mA within 2θ degrees range of 5° to 90°. The surface morphological analysis was carried out using the Zeiss Merlin VP Compact scanning electron microscope at an accelerating voltage of 0.5kV.

Modelling and statistical analysis

Design Expert version 13 software was employed in modelling, analysing, and optimising data in this study. The data collected for both acetic and citric acids were fitted to the regression model described by equation (3) (Onukwuli and Nnanwube, 2022; Khodaei et al., 2022; Golaghaei et al., 2024).

$$Y = \beta_o + \sum_{i=1}^{n} \beta_i X_i + \sum_{i=1}^{n-1} \sum_{j=i+1}^{n} \beta_{ij} X_i X_j (i \neq j) + \sum_{i=1}^{n} \beta_{ii} X_i^2 + \varepsilon, (3)$$

where Y represents the response, β_o, β_i, β_{ii}, and β_{ij} are the constant, linear, quadratic, and interaction coefficients respectively, X_i and X_j are independent variables, where $i \neq j$, ε is the error term, and n is the number of factors.

The fitting of the regression models for the percentage of silver leached in acetic and citric acid systems was done by first comparing the experimental mean values of each term when added sequentially. This fitting was based on a significance criterion at 95% confidence level (p-value < 0.05), lack of fit at p-value > 0.05, high adjusted R^2, and low standard deviation. Notably, cubic and higher-order interactions were eliminated because the experimental runs were not enough to estimate all the coefficients. Consequently, the quadratic model was identified as the best fit. This model was proven to be adequate and reliable via diagnostic analysis of predicted and actual experimental data.

Analysis of variance (ANOVA) was used to investigate the significance of the selected leaching factors (model terms) and their interactions on the percentage of silver leached, applying the same significance criteria for the model. In general, insignificant model terms, unless necessary for hierarchy, are omitted to improve the model (Raeisi et al., 2023; Salahi et al., 2023). However, in this study, all insignificant terms were maintained, and their effects alongside all significant terms were further investigated using the response surface plots. This information, as well as inherent characteristics of the leaching reactions and constraints were then employed to optimise the silver leaching process via ramp technique by applying the software's built-in gradient descent, numerical optimisation algorithm, and desirability function.

Results and discussion

XRF and XRD analysis

Table 2 shows the elemental composition of the WPCB sample by XRF analysis. Iron, silicon, and copper are identified to predominantly make up the WPCB sample with respective concentrations of 35.27 wt%, 25.9 wt%, and 13.3 wt%. Silver, which is the primary target of this study, takes up only 1.06 wt% of the total elements within the sample. The results also indicated the presence of other components, including significant quantities of aluminium, calcium, bromine, and traces of other metals such as tin, zinc, and nickel, which are classified as others. Notably, these identified elements are in line with previously reported results on the elemental characterisation of WPCB, but with different percentage compositions (Wang et al., 2015; Khayyam Nekouei et al., 2019; Ichikawa et al., 2023). The difference in compositions may be attributed to the difference in type, brand, model, and year of manufacture of the electrical components selected by the individual studies (Petter et al., 2015).

Table 2. *Elemental composition of the WPCB by XRF analysis*

Elements	Composition (wt%)
Fe	34.27
Si	25.9
Cu	13.03
Al	9.18
Ca	4.82
Br	3.15
Ag	1.06
Others	8.59

The XRD analysis was used to ascertain the XRF findings and most importantly, identify the form (mineralogy) in which the various elements, particularly silver, are present in the WPCB sample. The identification of the various forms in which the individual element in the sample is present is imperative, as it directly influences their relative selectivity. The result of the XRD analysis is shown in Figure 2. The diffraction pattern reveals sharp and distinct peaks corresponding to several metal phases, including copper, and silver, along with minerals, including schapbachite ($AgBiS_2$), sphalerite ((Zn, Fe) S), quartz (SiO_2), siderite ($FeCO_3$), alarsite ($AlAsO_4$), and chabazite ($CaAl_2Si_4O_{12}{\cdot}6H_2O$). These phases correspond to the various materials used in the manufacturing of printed circuit boards and confirm the presence of the elements indicated by the XRF analysis.

The most prominent peaks in the XRD pattern at diffraction angles of 43.3° and 55.5° correspond to metallic copper, whereas

the peaks at diffraction angles of 38.5° and 78.4° are attributed to metallic silver and silver in the form of schapbachite. Both copper and silver, in their metallic forms, can easily undergo dissolution in acids. Their coexistence in the WPCB could potentially present some challenges during the process of leaching silver, particularly regarding selectivity, as both metals may dissolve concurrently. Nonetheless, selective leaching of silver is possible under controlled conditions. Other crystalline phases, such as chabazite, sphalerite, alarsite, siderite, and quartz, represent non-metallic or trace components of the WPCB.

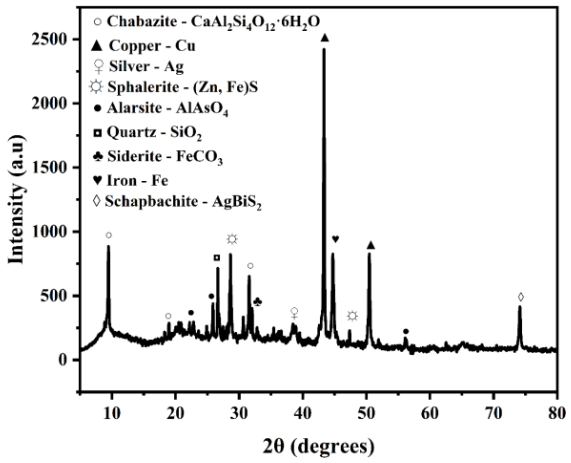


Fig. 2. XRD spectra of the WPCB

SEM Analysis

The SEM analysis was conducted to identify the form, shape, and surface features of the mechanically reduced particles within the WPCB, all of which are essential in understanding how the material will behave during the leaching process. Figure 3 shows the SEM micrograph of the WPCB sample used in this study. The micrograph reveals a heterogeneous structure, where different sizes of metallic and non-metallic particles are dispersed. The presence of metallic silver and copper, and metallic mineral schapbachite, identified in earlier XRF and XRD analyses, is evidenced by the bright grey regions (Yin et al., 2011). These regions are not uniformly distributed, which could lead to localised variations in the percentage of metals leached, particularly silver. Areas that are dense with metallic particles are likely to experience higher rates of leaching, provided the lixiviant reaches these concentrated regions. Some of these metallic particles appear as irregularly shaped particles, exhibiting rough and uneven surfaces with numerous pores. The irregularity and roughness of these metallic particles are key considerations, as they provide more active sites for the lixiviant to interact with the metal, potentially enhancing the leaching process. The remaining metallic portions consist of predominantly smooth and mechanically fragmented particles, with a mixture of clustered and individual cylindrical shapes, as shown in Figure 3. The somewhat smooth nature of the particles would provide a more uniform distribution of lixiviant, but often with less intensity relative to rough surfaces. Moreover, the clustered-rich regions would reduce the available surface area that comes into direct contact with the lixiviant. Consequently, a low percentage of metal may be leached.

Further examination of the micrograph shows irregular and cylindrical-shaped particles, with a distinctive dark grey colour. The majority of these particles can be identified as glass fibres encapsulated with resins containing quartz, sphalerite, alarsite, and siderite (Nekouei et al., 2018; Zhu et al., 2020). These materials are generally inert under mild acid-leaching conditions and will not interfere with the recovery of silver. However, their presence shows the complexity of the WPCB matrix, which consists of various metallic and non-metallic materials tightly integrated into one another.

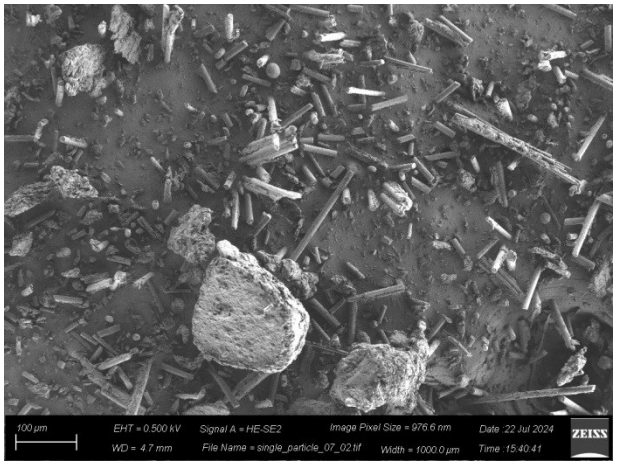


Fig. 3. SEM micrograph of the WPCB sample of particle sizes <150µm at 100µm before leaching

Regression models, analysis of variance, and response surface plots

Table 3 presents the experimental results for the runs generated from the selected ranges of temperature, lixiviant concentration, and leaching time. The quadratic models with coded coefficients for the percentage of silver leached in acetic and citric acid are presented in equations (4) and (5). The adjusted R^2 and standard deviations were 0.8840 and 1.08 for equation (4) and 0.9978 and 0.20 for equation (5).

$$\%\ Silver\ leached\ (Acetic\ acid) = 9.54 + 0.61A - 1.15B + 2.38C + 0.41AB + 0.1AC + 2.05BC - 2.65A^2 - 0.77B^2 - 0.91C^2 \quad (4)$$

$$\%\ Silver\ leached\ (Citric\ acid) = 15.48 + 0.97A - 1.82B - 0.98C - 1.34AB - 0.61AC + 1.71BC - 5.26A^2 - 0.57B^2 - 1.52C^2 \quad (5)$$

The terms A, B, and C are the leaching factors: leaching temperature, lixiviant concentration, and leaching time, respectively.

Table 4 presents the ANOVA results for the quadratic model of silver leaching in citric acid (Equation (5)). The overall model is significant, with a p-value below the significance level of 0.05 (p-value < 0.0001) and a corresponding F-value of 942.47. The model also exhibited a non-significant lack of fit (p-value = 0.0535 and F-value = 1.91). This means the model fits well with the experimental data. All the model terms are significant with p-values < 0.0001. This indicates that the factors considered for this study and their interactions significantly affect the leaching process in one way or another. The order of significance based on the F-values is as follows: A^2 > B > C^2 > BC > AB > C > A > B^2 > AC. Table 4 also presents the ANOVA results for the quadratic models of silver leaching in acetic acid. As expected, the model (p-value = < 0.0001, F-value = 17.08) and its lack of fit (p-value = < 0.0706, F-value = 4.20) are statistically significant and insignificant, respectively.

Table 3. *RSM-CCD experimental design with process parameters and corresponding percentage of silver leached in acetic and citric acid*

Run	Temperature (°C)	Lixiviant concentration (M)	Leaching time (h)	Silver leached in acetic Acid (%)	Silver leached in citric Acid (%)
1	50	2	3	11.48	15.30
2	50	2	0.6	3.28	12.84
3	50	2	3	9.84	15.30
4	50	2	5	9.84	8.61
5	50	2	3	9.84	15.30
6	30	3	2	4.92	8.47
7	50	4	3	9.84	10.11
8	50	2	3	9.84	15.30
9	80	1	2	3.28	13.39
10	30	1	4	6.56	7.92
11	50	2	3	9.84	15.30
12	50	2	3	9.84	14.89
13	30	3	4	11.48	9.70
14	90	2	3	4.92	3.14
15	80	3	4	11.48	3.55
16	30	1	2	4.92	12.16
17	50	0.3	3	4.92	15.98
18	25	2	3	4.92	9.29
19	80	1	4	3.28	7.10
20	80	3	2	3.28	4.37

The linear terms B and C, curvature effects A^2, B^2, and C^2, and the interaction term BC are all significant model terms with p-values < 0.05, and their order of significance based on their corresponding F-values is C > A^2 > BC > B > C^2 > B^2. Conversely, the underlined linear term A and interaction terms AB and AC have p-values > 0.05 and are therefore not considered significant. In this regard, acetic acid concentration and leaching time are the only factors that greatly affect the silver leaching process, while temperature does not. In addition, the former is dependent on each other, but neither depends on the latter.

The three-dimensional (3D) response surface plots are the graphical representation of a response as a function of two independent variables while maintaining all other variables constant. The plots help understand the main and interaction effects by facilitating a straightforward analysis of the independent variables. The shape of the 3D surfaces shows the magnitude of the correlation between the independent variables and the response, with the colours blue, green, yellow, and red of the response surface plots indicating the strength of these effects in ascending order (Dzikunu et al., 2024).

In Figure 4, the three-dimensional (3D) response surface plots for the percentage of silver leached in acetic acid are visualised. The 3D surface plot in Figure 4(a) shows the relationship between temperature and concentration of acetic acid and exhibits a quadratic shape. At lower temperatures, the percentage of silver leached rises, but as temperature increases, the percentage of silver leached decreases, as also shown in Figure 4(c). While temperature exhibits this effect, it is not statistically significant under the conditions tested. Notwithstanding, this does not imply temperature is unimportant; rather, its effect may be complex and possibly intertwined with other variables, for example, the curvature effect (A2). The percentage of silver leached, on the other hand, increases with increasing acetic acid concentration until reaching a saturation point (Figure 4(a) and (e)). This effect is more pronounced at higher concentrations around the turning points of the temperature curve and at higher leaching times, indicated by the dark yellow colour. As shown by Figure 4(c), increasing the leaching time increases the percentage of silver leached, and it is more substantial at higher leaching times around the turning points of the temperature curve (dark yellow colour in the 3D surface plot). The leaching time while interacting with acetic acid concentration also showed an increasing percentage of silver leached effect that is about 86% of the lone effect of leaching time, with the largest percentage of silver leached at higher concentrations and extended time, as seen in Figure 4 (e).

Table 4. *Analysis of variance (ANOVA) for the quadratic models for the percentage of silver leached in acetic and citric acids*

Source	Acetic Acid					Citric Acid				
	Sum of Squares	df	Mean Square	F-value	p-value	Sum of Squares	df	Mean Square	F-value	p-value
Model	179.16	9	19.91	17.08	< 0.0001	345.62	9	38.40	942.47	< 0.0001
A-Leaching Temperature	2.61	1	2.61	2.24	0.1652	6.60	1	6.60	161.91	< 0.0001
B-Lixiviant Concentration	16.76	1	16.76	14.39	0.0035	42.50	1	42.50	1043.06	< 0.0001
C-Leaching Time	62.18	1	62.18	53.36	< 0.0001	10.44	1	10.44	256.27	< 0.0001
AB	1.37	1	1.37	1.18	0.3036	14.70	1	14.70	360.84	< 0.0001
AC	0.0572	1	0.0572	0.0491	0.8292	1.98	1	1.98	48.51	< 0.0001
BC	21.50	1	21.50	18.45	0.0016	14.93	1	14.93	366.42	< 0.0001
A^2	45.60	1	45.60	39.14	< 0.0001	179.86	1	179.86	4414.11	< 0.0001
B^2	11.94	1	11.94	10.25	0.0095	6.59	1	6.59	161.73	< 0.0001
C^2	12.78	1	12.78	10.97	0.0079	35.80	1	35.80	878.56	< 0.0001
Residual	11.65	10	1.17			0.4075	10	0.0407		
Lack of Fit	9.41	5	1.88	4.20	0.0706	0.2675	5	0.0535	1.91	0.2471
Pure Error	2.24	5	0.4479			0.1399	5	0.0280		
Cor Total	190.81	19				346.03	19			

This demonstrates that the effect of the concentration of acetic acid is dependent on the leaching time, as confirmed by the ANOVA results in Table 4.

Similarly, in Figure 4, the 3D response surface plots for the percentage of silver leached in citric acid are illustrated. The temperature appears to follow a similar trend as when silver was leached in acetic acid. However, the effect is significant and stronger across all leaching times and concentrations around the turning points of its curve, as indicated by the dark red colour in Figure 4 (b) and (d). On the other hand, the concentration of citric acid and leaching time show diminishing effects on the silver dissolution process. Increasing both the concentration and leaching time as lone or interacting factors decreases the percentage of silver leached, as shown in Figure 4(b), (d), and (f). When interacting with each other, the effect is more pronounced at lower values (dark red colour in Figure 4 (f)).

It is important to note that the observed effects and associated yield of the response surface plots are a result of the nature of the underlying leaching reactions, particularly the chemical characteristics inherent to the reactant and product species. For a better understanding of these behaviours, one-factor graphical representations are used to evaluate the leaching system under the conditions tested for both acetic and citric acids, based on possible dissolution reactions in subsequent sections.

Studies of silver dissolution in acetic acid

Possible reaction mechanism for the silver dissolution in acetic acid

Organic acids have been reported to undergo two main processes when dissolving minerals from ores; acidification and complexation (Jadhav et al., 2016b). During acidification, the acid dissociates in an aqueous medium to supply protons and ligands. The protons are reduced to oxidize the metal of interest from its ore. The presence of oxidants such as oxygen and hydrogen peroxide render this process more readily. Conversely, the ligand reacts with the metal ion to form a more stable and soluble complex in the complexation reaction. Based on these two processes, the reaction steps for the dissolution of silver in acetic acid can be described by equations (6) – (9). The dissociation of acetic acid in aqueous medium can be written as:

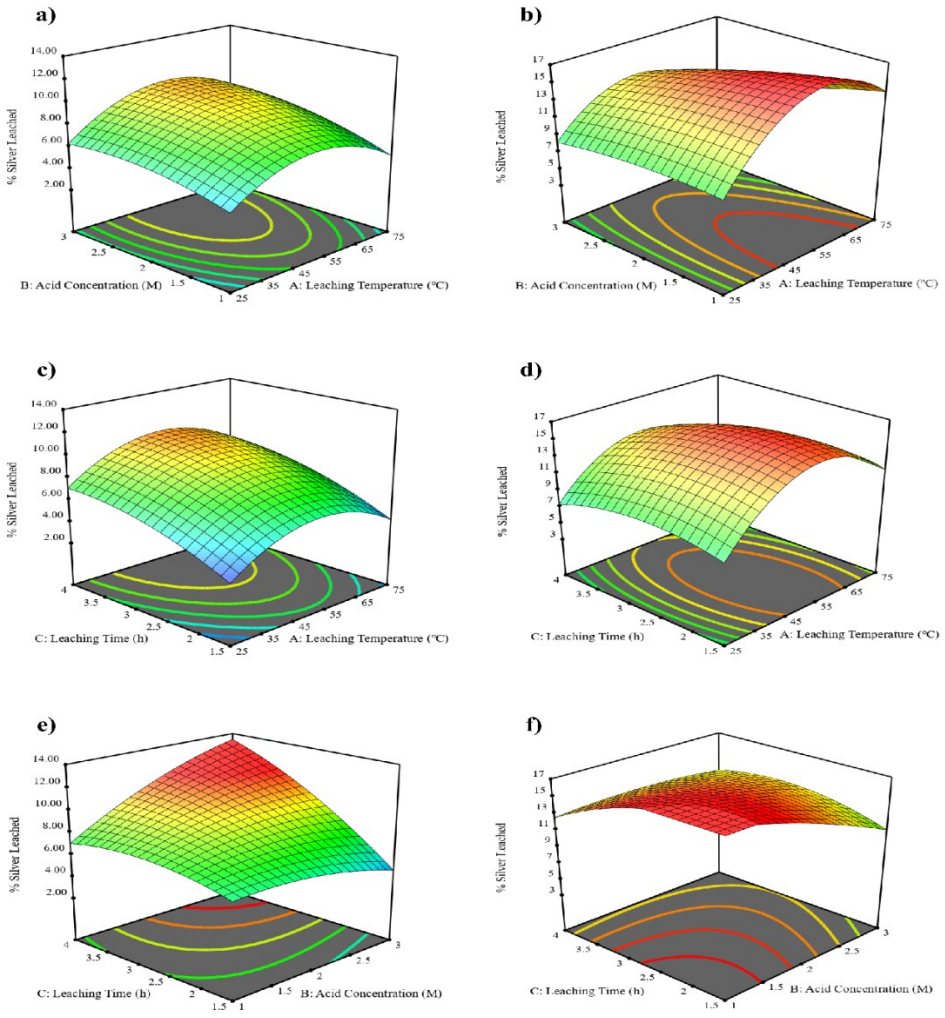


Fig. 4. 3D response surface plots showing effects of two-factor interactions on the percentage of silver leached in acetic and citric acid respectively: (a) and (b) leaching temperature versus acid concentration, (c) and (d) leaching temperature versus leaching time, and (e) and (f) acid concentration versus leaching time.

$$CH_3COOH + H_2O_{(l)} \leftrightarrows CH_3COO^-_{(aq)} + H_3O^+_{(aq)} \quad (6)$$

Based on the chemical composition of the WPCB sample used in this study, the following dissolution reaction is possible with atmospheric oxygen as an oxidant.

$$4Ag_{(s)} + O_{2(g)} + 4H_3O^+_{(aq)} \rightarrow 4Ag^+_{(aq)} + 6H_2O_{(l)} \quad (7)$$

A more soluble complex is formed by a complexation reaction between the ionic species and the ligand from acetic acid, as shown in equation (8).

$$Ag^+_{(aq)} + CH_3COO^-_{(aq)} \rightarrow AgCH_3COO_{(aq)} \quad (8)$$

Consequently, the overall leaching reaction can be written as:

$$4Ag_{(s)} + 4CH_3COOH + O_{2(g)} \rightarrow 4AgCH_3COO_{(aq)} + 2H_2O_{(l)} \quad (9)$$

Effects of process parameters on the silver dissolution

Effect of temperature

Figure 5 shows the effects of the individual factors on the percentage of silver leached in acetic acid. The effect of temperature on the leaching of silver is depicted in Figure 5(a). It can be observed that the percentage of silver leached increased from 6% to about 10% when the temperature initially increased from 25°C to approximately 53°C. The percentage of silver leached decreased to 7% as the temperature was further increased to 75°C. Aydoğan et al. (2024) observed a similar trend at a higher temperature (61.5°C) using hydrogen peroxide as an oxidant, attributing this behaviour to the decomposition of the peroxide. However, in this case, the temperature behaviour may be linked to the solubility of atmospheric oxygen, which decreases with increasing temperature (Hao et al., 2022). Thus, at temperatures below 53°C, oxygen was readily dissolved, increasing the available oxygen for oxidizing the silver, and vice versa for temperatures above 53°C. In addition, while the reactivity of silver is aided at higher temperatures, the reactivity of other metals, such as copper in this case, is relatively higher. Consequently, the acidification and complexation of these

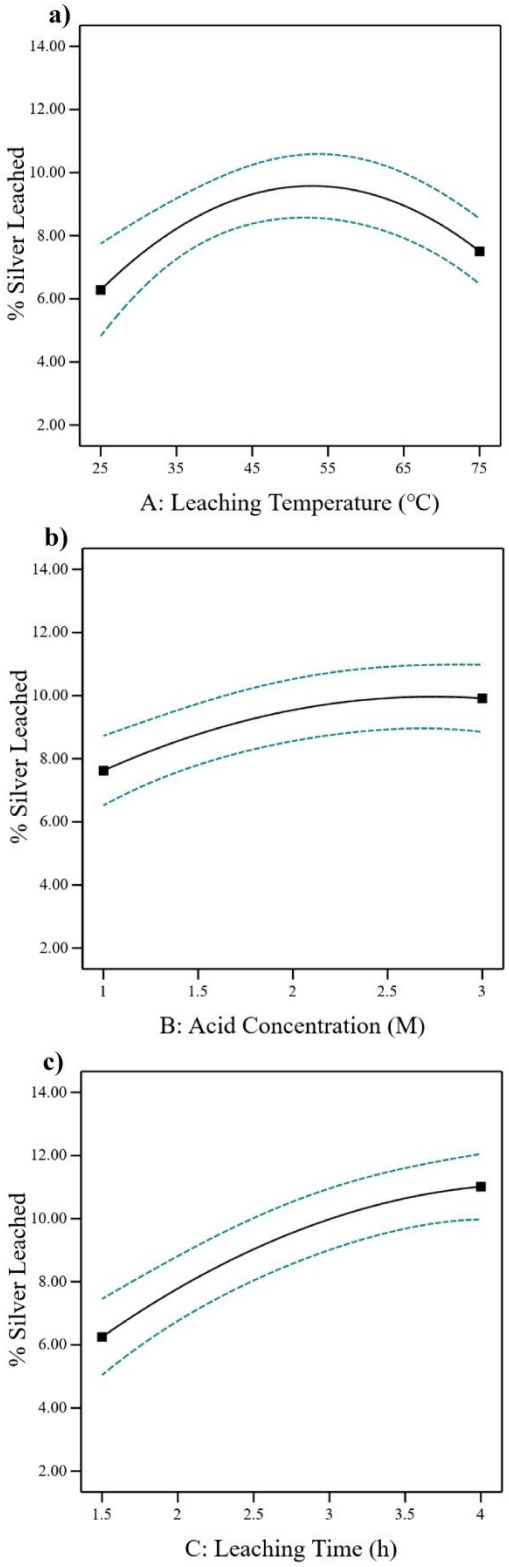


Fig. 5. The effect of (a) leaching temperature at 2 M and 2.75 h, (b) acetic acid concentration at 50°C and 2.75 h, and (c) leaching time at 50°C and 2 M on the percentage of silver leached in acetic acid

metals might be more pronounced, thereby decreasing the percentage of silver leached. Despite this temperature-dependent trend, the statistical analysis (Table 4) indicated that the temperature range tested was statistically insignificant relative to acetic acid concentration and leaching time, as it recorded a p-value > 0.05. This suggests that the dissolution process may occur at a favourable rate in the range of acetic acid concentration and leaching time tested irrespective of temperature in the studied temperature range.

Effect of acetic acid concentration

The effect of the concentration of acetic acid on the percentage of silver leached is shown in Figure 5(b). The concentration of acetic acid exhibited positive behaviour on the percentage of silver leached. Initially, the percentage of silver leached rose slowly before reaching a plateau at 2.5 M. Thereafter, the silver extraction remained significantly the same, with about 10% as the maximum percentage of silver leached. As the concentration increased from 1 M to 2.5 M, more hydroxonium (H_3O^+) and acetate ions (CH_3COO^-) were released into the solution, increasing the oxidation and complexation reactions of silver (Suanon et al., 2016). However, at 2.5 M concentration, all available silver ions may have already formed complexes with acetate ions. Thus, the percentage of silver leached remains relatively constant beyond this point regardless of the increasing concentration of acetate ions in the solution.

Effect of leaching time

The effect of leaching time on the percentage of silver leached using acetic acid is presented Figure 5(c). The leaching of metals has consistently been proven to be time-dependent (Preetam et al., 2022). Similarly in this study, the silver dissolution time in acetic acid was found to be the most significant factor, as indicated by the ANOVA (Table 4) and response surface analysis (Figure 4). As shown in Figure 5(c), the percentage of silver leached increased sharply with increasing the leaching time to a maximum of 11% in 4 hours. This is attributed to the fact that higher leaching times allowed for more interaction between the acetic acid, the atmospheric oxygen, and the silver. Simultaneously, this implies that silver dissolution takes a longer time to reach completion.

Optimisation of the leaching factors/parameters

From hydrometallurgical principles, increasing the operating temperature, lixiviant concentration and leaching time are expected to increase the metal yield. This suggests that the most effective way to achieve the highest metal yield is to maintain these process parameters at higher levels. In practice, leaching systems vary from one another and may not always conform to expected behaviour, however, a higher metal yield is desired. While achieving a higher yield is desired, it is equally important to consider the economic viability and environmental sustainability of the leaching system, hence, the necessity of the optimisation of the process parameters.

In the present study, the optimisation of the silver-acetic acid leaching process was based on costs associated with the consumption of acetic acid and energy since the acid is eco-friendly. As previously established, temperature might not have a significant effect on the leaching process. Moreover, the percentage of silver leached reduces at temperatures above 53°C. Increasing leaching time, on the other hand, continuously increases the percentage of silver leached, and increasing the concentration also increases the percentage of silver leached until reaching saturation at 2.5 M. Generally, if the concentration required is higher, the cost of the acid is also higher.

Similarly, higher temperatures and longer leaching time invariably led to a greater energy (heating) cost. Comparatively,

the cost associated with the consumption of energy is much greater than that of the acetic acid. In these regards, the constraints imposed for the optimisation of the leaching process were temperature minimisation, lixiviant concentration range limitation (1-2.5 M), and percentage of silver leached maximisation. No constraint was placed on the leaching time since a minimisation constraint was placed on temperature.

The results of the optimisation of the process parameters used in studying the leaching of silver in acetic acid are displayed in Figure 6. The optimum values for temperature, lixiviant concentration, and leaching time to achieve the highest possible percent silver leached (11.48%) at low energy cost were determined to be 38.8°C, 2.5 M, and 4 hours. The desirability value of 0.851 suggests that the optimal values determined meet the constraints imposed on the leaching system.

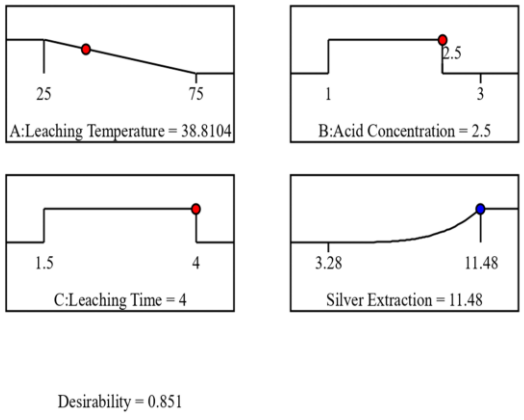


Fig. 6. Optimum leaching conditions suggested for achieving the highest possible percentage of silver leached in acetic acid at low cost

Kinetic studies of the silver-acetic acid leaching process

Shrinkage core models

The leaching reactions of solid particles with reagents are predominantly heterogeneous and can generally be expressed as: $aA_{fluid} + bB_{solid} \rightarrow$ products. The kinetics of solid particles interacting with reagents can be described by several heterogeneous models. Notwithstanding, the shrinkage core models (SCMs) are often used to describe this interaction. SCMs describe the reaction between the solid particle, assumed to be a perfect sphere, and the fluid to occur at the outer surface of the solid. Initially, the reactant species from the reagent is carried through the bulk fluid to the surface of the solid sphere particles via mass transport, kickstarting the reaction. As the reaction proceeds, the unreacted core shrinks towards the particle centre while a porous product layer, with increasing thickness, forms around it (Wu et al., 2015; Habbache et al., 2017). The slowest process of the overall reaction is the rate-determining step, hence, considered to control the overall reaction.

When the overall reaction is controlled by the surface chemical reaction (CR) occurring at the solid/fluid interface, equation (10) is used to describe the leaching kinetics.

$$1 - (1 - \alpha)^{\frac{1}{3}} = k_c t \qquad (10)$$

Similarly, when diffusion through the product layer (DPL) is the rate-controlling step, equation (11) can be used to describe the dissolution kinetics.

$$1 - \frac{2}{3}\alpha - (1 - \alpha)^{\frac{2}{3}} = k_p t \qquad (11)$$

Furthermore, when diffusion through the liquid film (DFL) controls the overall reaction, the leaching kinetics can be described using equation (12) (for particle sizes greater than 0.1 mm) (Levenspiel, 1998; Free, 2022a).

$$1 - (1 - \alpha)^{\frac{1}{2}} = k_f t \qquad (12)$$

where α is the fraction of the silver leached, t is the leaching or reaction time, and k_c, k_p, and k_f, are the apparent rate constants for the chemical reaction, diffusion through the product layer, and diffusion through the liquid film-controlled models respectively.

To determine the rate-limiting step of the leaching reaction, in this case, silver-acetic acid leaching reaction, the functions of the fraction of silver reacted were plotted against the reaction time, t, for different temperatures and constant concentration. The plotted points were linearly fitted, and the respective regression coefficients (R^2) were evaluated. Moreover, the apparent rate constants were determined from the slopes of the linear fits.

The kinetic plots according to the SCMs for the silver-acetic acid leaching system at 30°C, 40°C, and 50°C are shown in Figure 7. These temperatures were chosen for the kinetic studies due to the optimum temperature value (38.8°C) falling below 50°C. Moreover, the effect of the initial temperature range (25°C - 75°C) tested was indicated by the ANOVA results (Table 4) to be insignificant. The results from the kinetic plots are also summarised in Table 5. As shown in Table 5 and Figure 7(a), the CR model recorded R^2 values of 0.9552, 0.9568, and 0.9583 for 30°C, 40°C, and 50°C, respectively. Similarly, in Figure 7(b), it can be observed that the DPL model exhibited R^2 values of 0.9823, 0.9801, and 0.9801 for 30°C, 40°C, and 50°C, respectively. Furthermore, according to the fitted results for the DFL model in Figure 7(c), R^2 values of 0.9547, 0.9563, and 0.9579 were recorded at 30°C, 40°C, and 50°C, respectively.

Comparing all the fitted results for the silver-acetic acid leaching data for temperature, all the models demonstrated a good fit. Nevertheless, the DPL model shows the best fit, as it recorded the highest R^2 values at all temperatures. This suggests that the kinetics of the silver-acetic acid leaching system might be better explained by the DPL model. Thus, the leaching process is likely controlled by the diffusion of the reactants and product species (equations (6) and(7)) through the product layer at these temperatures. The effects of concentration on kinetic behaviour were also studied, with the corresponding leaching apparent rate constants and R^2 values of the fitted models summarised in Table 5.

Activation energies evaluation

In general, diffusion-controlled processes are less sensitive to temperature, unlike chemical-controlled processes (Clotilde Apua and Madiba, 2021).

Table 5. *Kinetic parameters and correlation coefficients evaluated from the various SCMs for the leaching of silver in acetic acid*

Process parameters	Surface chemical reaction		Diffusion through the product layer		Diffusion through liquid film	
	K_c (h^{-1})	R^2	K_p (h^{-1})	R^2	K_f (h^{-1})	R^2
Temperature (K)						
303	0.0064	0.9552	0.00029	0.9823	0.0095	0.9547
313	0.0066	0.9568	0.00036	0.9801	0.0097	0.9563
323	0.0068	0.9583	0.0004	0.9801	0.0099	0.9579
CH3COOH Conc. (M)						
1	0.00093	0.2993	0.00004	0.2913	0.0014	0.2994
2	0.0068	0.9583	0.0004	0.9801	0.0099	0.9579
3	0.0126	0.9889	0.0008	0.9985	0.0186	0.9885

Given that the kinetics of the silver-acetic acid leaching system might be well-described by the DPL model, it is important to elucidate its applicability based on the temperature sensitivity. The activation energy is the parameter that quantifies the temperature sensitivity of reactions - equation (13). Therefore, in this study, the linearized Arrhenius model expressed in equation (14) was used to evaluate the activation energy of the silver-acetic acid leaching reactions based on the SCMs.

$$k_p = \upsilon \, exp\left(-\frac{E_a}{RT}\right) \quad (13)$$

$$ln\, k = ln\, \upsilon - \frac{E_a}{R}\left(\frac{1}{T}\right) \quad (14)$$

Where k is the apparent rate constant, υ is the pre-exponential (frequency) factor, E_a is the activation energy, R is the universal gas constant (8.314 J/(mol.K), and T is the reaction temperature. By generating a straight line from the plots of lnk against 1/T for the individual models, the activation energies were calculated from the slope (E_a = -R × Slope).

Figure 8 depicts the Arrhenius plots of the individual SCMs, and Table 6 summarises information on the activation energy and coefficient of correlation (R^2). All the SCMs fit well with the Arrhenius model, with R^2 values of 0.9999, 0.9686, and 0.9998 for the CR (Figure 8(a)), DPL (Figure 8(b)), and DFL (Figure 8(c)), respectively. This indicates that the activation energies obtained from the slopes of the fits can be considered accurate and can be used to determine the temperature sensitivity of the respective models. Nonetheless, the DPL model showed the lowest R^2 value among the SCMs. This result deviates from the expected kinetic data fitting of the SCMs, which previously exhibited the highest R^2 value, which suggested that it may best explain the kinetics of the leaching system. In this regard, the selection of the most suitable model was ultimately guided and made clearer by the corresponding activation energies of the SCMs.

The CR model exhibited a low activation energy of 2.46 kJ/mol, as shown in Table 6. Thus, a low amount of energy is required to transport the oxygen and acetic acid molecules (equation (9)) to the outer skin of the silver-containing particles to cause the leaching reaction.

Table 6. *Kinetic parameters from the Arrhenius plots based on the SCMs for silver leaching in acetic acid*

Kinetic parameters	Chemical reaction	Diffusion through product layer	Diffusion through liquid film
Activation Energy, E_a (kJ/mol)	2.46	13.13	1.68
Coefficient of correlation (R^2)	0.9999	0.9686	0.9998

This significantly deviates from the typical energy requirement of a chemically controlled process because they generally demand higher energy input and therefore are temperature dependent. Hence, the CR model may not be used to accurately describe the kinetic behaviour of the silver-acetic acid leaching system.

Again, unlike chemically controlled processes, which generally have activation energies of more than 40 kJ/mol, diffusion-controlled processes exhibit lower activation energies (less than 20 kJ/mol) (Faraji et al., 2022). In Table 6, it can also be observed that the DFL model recorded a relatively low activation energy value of 1.68 kJ/mol. While this activation energy value aligns with the typical energy requirement for a diffusion-controlled process, it is unusually low. A very low activation energy for the DFL model implies that the transport of acetic acid and oxygen through the liquid film surrounding the solid silver particles, occurs with almost no resistance. In practice, the diffusion of species through the liquid film would encounter resistance such as viscosity and concentration gradient, particularly when the reactant species involve CH_3COOH, a weak acid. The presence of such a reactant, which must dissociate and diffuse through the liquid film and reach the silver surface, would inherently require a moderate amount of energy to overcome these resistances (Jansson, 1980). This suggests that the DFL model may not be the rate-determining step of the silver-acetic acid leaching system.

The DPL model, on the other hand, exhibited relatively high activation energy (13.13 kJ/mol). This follows the expected activation energy requirement for diffusion through the product layer-controlled process.

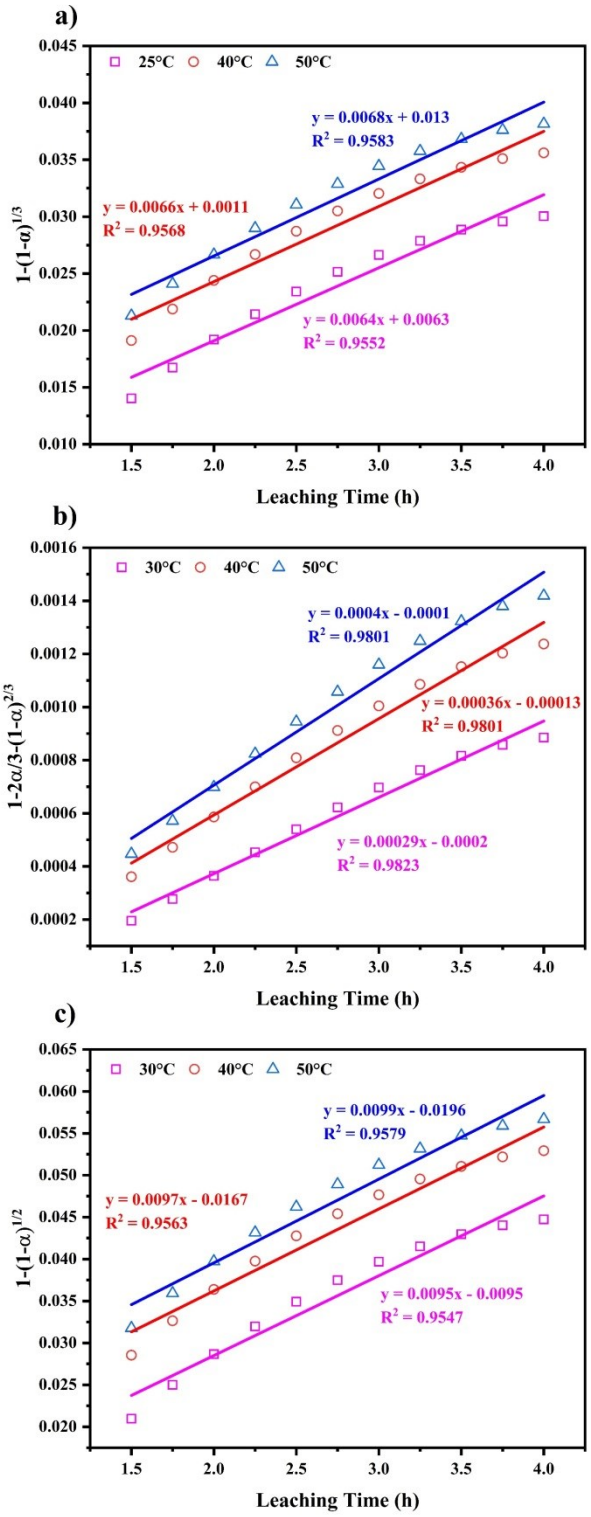


Fig. 7. SCM plots for silver leaching in 2 M acetic acid: (a) Surface chemical reaction model [1-(1-α)$^{1/3}$], (b) Diffusion through the product layer [1-2α/3-(1- α)$^{2/3}$], and (c) Diffusion through the liquid film [1-(1- α)$^{1/2}$] at 30°C, 40°C, and 50°C.

This further ascertains that the silver-acetic acid leaching system is controlled by the diffusion through the product layer, hence, the DPL model can be used to accurately describe the kinetic behaviour of the leaching reaction.

The final empirical model for describing the kinetic behaviour of the silver-acetic acid leaching system was then

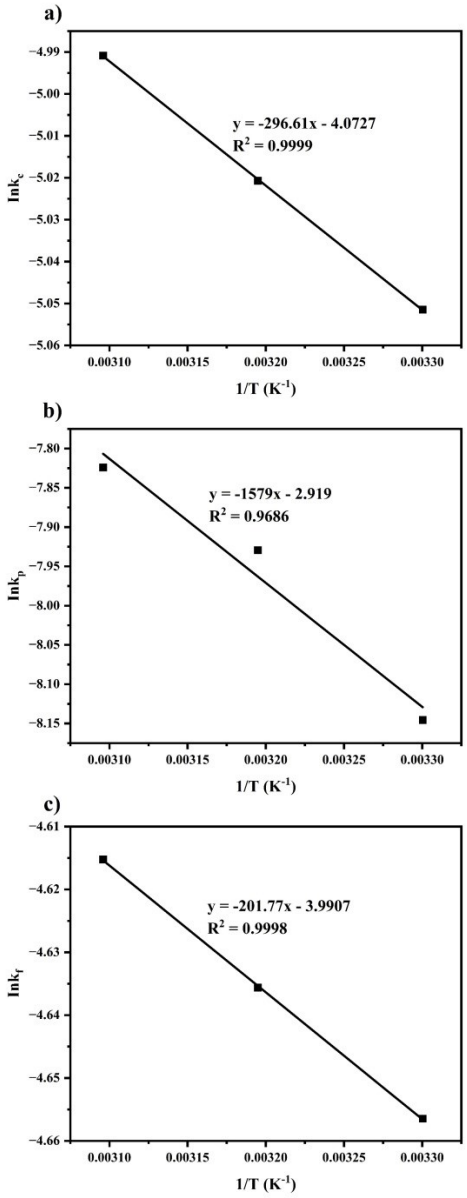


Fig. 8. Arrhenius plot for (a) Surface chemical reaction, (b) Diffusion through product layer, and (c) Diffusion through liquid models for the leaching of silver in acetic acid

derived by combining equations (11) and (13), and it is expressed in equation(15).

$$1 - \frac{2}{3}\alpha - (1-\alpha)^{\frac{2}{3}} = \upsilon \times C^{c} \times exp\left(-\frac{E_a}{RT}\right) \times t \quad (15)$$

where α, υ, E_a, R, T, and t have the same meanings from previous equations, C is the lixiviant concentration, and c is the reaction order with respect to the lixiviant concentration.

The reaction order was evaluated from the plot of lnk_p versus lnC as 2.7909 (Free, 2022; Dzikunu et al., 2024), whereas the pre-exponential factor, υ, was evaluated from the intercept of the DPL kinetic plot (Figure 8(b)) as 5.4 × 10^{-2} h^{-1}. The overall empirical kinetic model representing the silver leaching from WPCB in acetic acid is written in equation (16).

$$1 - \frac{2}{3}\alpha - (1-\alpha)^{\frac{2}{3}} = 5.4 \times 10^{-2} \times C^{2.7909} \times exp\left(-\frac{13.13\times10^{3}}{8.314T}\right) \times t \quad (16)$$

Studies of the silver-citric acid leaching process

Possible mechanism for the silver dissolution

As previously established for acetic acid, the dissolution of silver in citric acid also follows acidification and complexation processes. Additionally, the oxidation of the silver in the WPCB samples follows equation (7). However, the initial dissolution reaction differs significantly, and the reaction steps can be described by equation (17)–(23).

The dissociation of citric acid, a weak triprotic acid, occurs in three distinct stages, each corresponding to the release of one proton, and can be written as follows:

$$C_6H_8O_{7(s)} + H_2O_{(l)} \leftrightarrows C_6H_7O_{7(aq)}^- + H_3O_{(aq)}^+ \quad (17)$$

$$C_6H_7O_{7(aq)}^- + H_2O_{(l)} \leftrightarrows C_6H_6O_{7(aq)}^{2-} + H_3O_{(aq)}^+ \quad (18)$$

$$C_6H_6O_{7(aq)}^{2-} + H_2O_{(l)} \leftrightarrows C_6H_5O_{7(aq)}^{3-} + H_3O_{(aq)}^+ \quad (19)$$

The pKa values for the equilibriums described by equations (17), (18), and (19) are 3.1, 4.8, and 6.4, respectively (Larba et al., 2013). Since the pH value of acid used in this study was 4, the reaction was carried out according to equations (17) and (18). Therefore, the complexation reactions for silver can be represented as follows:

$$Ag_{(aq)}^+ + C_6H_7O_{7(aq)}^- \rightarrow AgC_6H_7O_{7(aq)} \quad (20)$$

$$Ag_{(aq)}^+ + C_6H_6O_{7(aq)}^{2-} \rightarrow AgC_6H_6O_{7(aq)}^- \quad (21)$$

The overall dissolution reaction can be written as:

$$4Ag_{(s)} + O_{2(g)} + 4C_6H_8O_{7(s)} \rightarrow 4AgC_6H_7O_{7(aq)} + 2H_2O_{(l)} \quad (22)$$

$$4Ag_{(s)} + O_{2(g)} + 4C_6H_7O_{7(aq)}^- \rightarrow 4AgC_6H_6O_{7(aq)}^- + 2H_2O_{(l)} \quad (23)$$

where Equations (22) and (23) represent the dissolution of metallic silver by the first and second dissociation of citric acid, respectively.

Effects of process parameters on the silver dissolution

Effect of temperature

Figure 9 presents the effects of the individual factors on the percent silver leached in citric acid. In Figure 9(a), the effect of temperature is visualised. As the temperature increased from 25°C, the percentage of silver leached increased sharply until about 54°C, where it began to drop as the temperature further increased. This behaviour was anticipated as previous studies have reported similar results (Yoğurtcuoğlu, 2023; Zan et al., 2024). Oxygen was readily dissolved as temperature increased, enhancing the oxidation of Ag to Ag^+. This was accompanied by a maximum of 16% silver leached at 54°C. When the temperature was higher, the solubility of oxygen decreased and resulted in less oxidation of the Ag. Moreover, the reactivities of metals such as copper increase at higher temperatures. As a result, they might have competed with the oxidised silver for the citrates, thereby reducing the silver extraction.

Effect of citric acid concentration

The effect of citric acid concentration on the percent silver leached is shown in Figure 9(b). It can be seen that the increase in the concentration of citric acid had a negative effect on the silver extraction, with the highest percentage of silver leached at about 17% observed at 1 M. Increasing the concentration beyond 1 M resulted in a consistent decrease in the percentage of silver leached. This result contrasts with those previously reported by other researchers who investigated a lower concentration range. Larba et al. (2013) observed an increase in metal dissolution with increasing concentration of citric acid from 0.01 M to 0.05 M while adding anions from NaCl, $NaNO_3$, and Na_2SO_4. Zan et al. (2024) and Yoğurtcuoğlu (2023) found a rather fluctuating behaviour with increasing concentrations while using an anion from NaCl and H_2O_2 as an oxidant, respectively. The current study, however, is consistent with the work of Li et al. (2010), who found that increasing the concentration of citric acid from 1.2 M to 1.5 M decreased the amount of metal leached. The decrease in silver dissolution with increasing citric acid concentration in the range tested can be due to the formation of copper oxide precipitates during the dissolution process, which creates a physical barrier between the silver ions and the citric acid (Barragan et al., 2020).

Effect of leaching time

The effect of leaching time on the percentage of silver leached is depicted in Figure 9(c). It is apparent that the leaching time, while having a notable influence, exhibited an inverse influence on the percentage of silver leached in citric acid for most times. As the leaching proceeded for 1.5 hours, the percent silver recorded for leached silver was 14.9%. Allowing the leaching to proceed for about 2 hours and 15 minutes increased the percentage of silver leached (15.6%) only slightly. Further increase in the leaching time resulted in a consistent decrease in the percentage of silver leached. From hydrometallurgical principles, increasing leaching time should increase the percentage of silver leached as it allows for progressive interaction between the citrate and silver ions until the point where all the citrate ions are consumed by the silver ions. However, the results of the current study demonstrate the opposite, such that a shorter time is enough to leach a relatively high percentage of silver from the metallic silver. This might be due to the reactivity of the other metals within the WPCB sample. Thus, the reactivity of silver, while relatively lower, may be enough for the silver to form complexes with citrate ions at shorter times. As the leaching time increases, other metals may become relatively more reactive, competing with the silver for the citrate ions, thereby decreasing the percentage of silver leached.

Optimisation of the leaching factors

The optimisation of the silver-citric acid system was carried out similarly to the silver-acetic acid system optimisation process. However, due to the difference in the behaviour of the leaching factors, the optimisation of the silver-citric acid leaching system was done under different constraints.

The constraints to achieve the maximum percentage of silver leached were leaching temperature, lixiviant concentration, and leaching time minimisation. Figure 10 shows the optimisation results for the silver-citric acid leaching process. The optimum values for temperature, citric acid concentration, and leaching time to achieve the highest possible percentage of

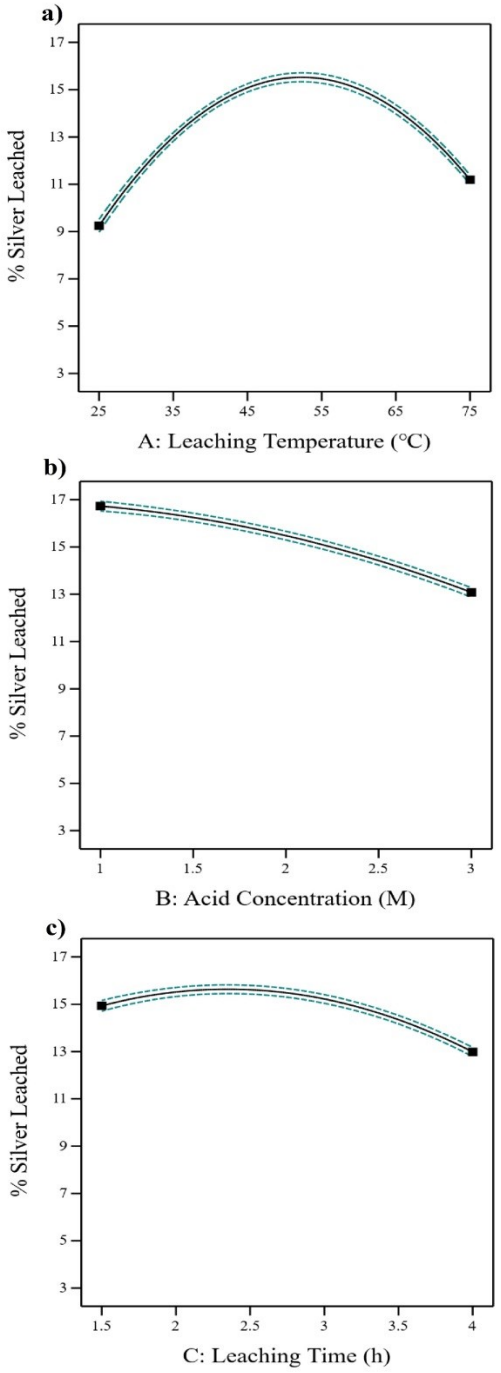


Fig. 9. The effect of (a) leaching temperature at 2 M and 2.75 h, (b) citric acid concentration at 50°C and 2.75 h, and (c) leaching time at 50°C and 2 M on the percentage of silver leached in citric acid

silver leached at low energy cost were determined at 37.7°C, 1 M, and 1.5 hours. The corresponding desirability value was 0.914, indicating that the optimum values determined meet the constraints imposed on the leaching system. Overall, the highest possible percentage of silver leached achieved at the optimal condition was 15.2%.

Kinetic studies of the silver-citric acid leaching process

Shrinkage core models

The kinetic behaviour of the silver-citric acid leaching reaction was investigated using shrinkage core models (SCMs)

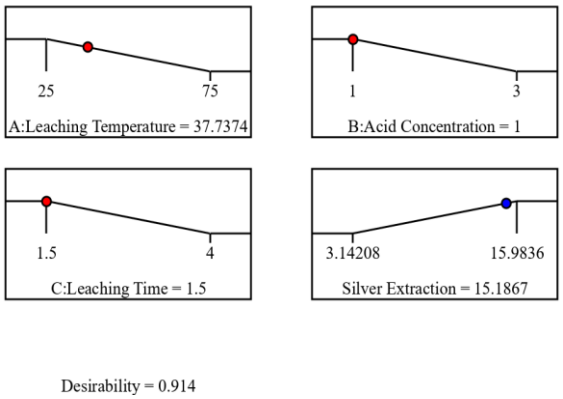


Fig. 10. Optimum leaching conditions suggested for achieving the highest possible percentage of silver leached in citric acid at low cost

expressed in equations (10), (11) and (12), within a temperature range of 30 to 50°C, a concentration range of 1 to 3 M, and a time range of 1.5 to 2.5 hours. The temperatures selected were based on the same criteria used for the kinetic studies of the silver-acetic acid leaching system. Similarly, the selection criteria for the time range were based on the optimum value (1.5 hours) identified through the optimisation process and the time that resulted in the highest percentage of silver leached. This choice is justified by the need to ensure sufficient reaction time for completion of the reaction while avoiding reactant depletion.

Figure 11 illustrates the SCM plots for the silver-citric acid leaching system at 30°C, 40°C, and 50°C. These plots are further summarised in Table 7, along with the effects of concentration on the kinetic behaviour. The CR model exhibited R^2 values of 0.9333, 0.9029, and 0.8481 at 30°C, 40°C, and 50°C respectively, as shown in Figure 11(a). As revealed by the DPL model plot in Figure 11(b), R^2 values of 0.9391, 0.9069, and 0.8508 were recorded at these respective temperatures. For the DFL model plot shown in Figure 11(c), the fits for the 30°C, 40°C, and 50°C indicate R^2 values of 0.9332, 0.9029, and 0.848, respectively. Considering the R^2 values collectively, all the models demonstrated satisfactory fit to the experimental data. This indicates that all the models can adequately describe the kinetic behaviour of the silver-citric acid leaching reaction. Notwithstanding, the DPL model might better explain the kinetic behaviour across these temperatures due to its relatively high R^2 values.

Activation energies evaluation

To justify the rate-determining step for the dissolution kinetics of leaching silver from WPCB in citric acid, indicated by the kinetic modelling analysis, the activation energies of the various models were evaluated using the plots generated from the Arrhenius equation (equation (14))). The results of the Arrhenius modelling of the SCMs, including the respective activation energies and correlation coefficients, are presented in Figure 12 and summarised in Table 8. The results show that R^2 values of 0.9932, 0.9973, and 0.9936 were recorded for the CR, DPL, and DFL models, respectively. Thus, all the SCMs showed over 99% fitting to the Arrhenius model, indicating that they highly follow the exponential dependence on temperature, and the evaluated activation energies can be accurately used to further analyse the SCMs. The DPL model, however, showed a relatively high R^2 value and may better explain the dissolution kinetics.

Table 7. *Kinetic parameters and correlation coefficients evaluated from the various SCMs for the leaching of silver in citric acid.*

Process parameters	Surface chemical reaction		Diffusion through the product layer		Diffusion through the liquid film	
	k_c (h^{-1})	R^2	$k_p \times 10^{-4}$ (h^{-1})	R^2	k_f (h^{-1})	R^2
Temperature (K)						
303	0.0039	0.9333	2.80	0.9391	0.0057	0.9332
313	0.0032	0.9029	2.69	0.9069	0.0047	0.9029
323	0.0025	0.8481	2.58	0.8508	0.0037	0.848
Citric acid Conc. (M)						
1	0.0026	0.8508	3.05	0.8532	0.0038	0.8507
2	0.0025	0.8481	2.58	0.8508	0.0037	0.848
3	0.0074	0.9812	5.88	0.9871	0.0109	0.981

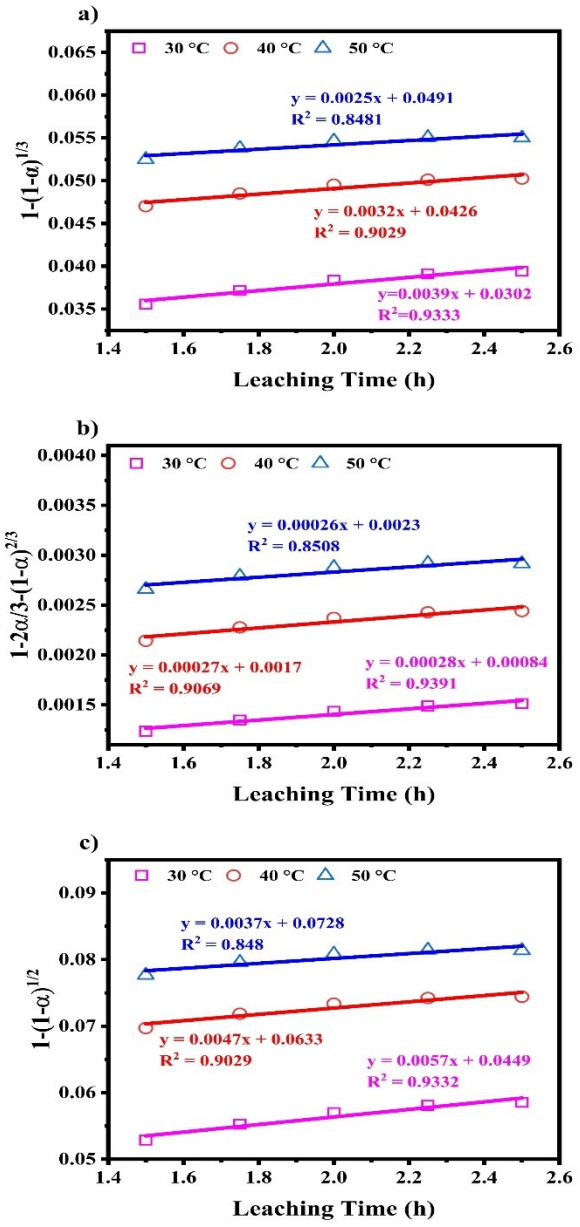


Fig. 11. SCM plots for silver leaching in citric acid: (a) Surface chemical reaction model [1-(1-α)$^{1/3}$], (b) Diffusion through the product layer [1-2α/3-(1- α)$^{2/3}$], and (c) Diffusion through the liquid film [1-(1- α)$^{1/2}$] at 30°C, 40°C, and 50°C

The activation energies recorded for the CR, DPL, and DFL are 18.06 kJ/mol, 3.29 kJ/mol, and 17.55 kJ/mol, respectively. The activation energy value evaluated for the CR model appears to contrast with the typical activation energy level for a chemically controlled reaction. For a chemical reaction to proceed, bonds between atoms or molecules must be broken and new bonds formed. Breaking bonds requires a significant amount of energy, which leads to a higher activation energy, often greater than 40 kJ/mol (Faraji et al., 2022; Tanaydin et al., 2022). The activation energy recorded for the CR model is less than 40 kJ/mol, creating an inconsistency with a typical chemically controlled process. Hence, the CR model cannot be used to describe the dissolution kinetics.

In contrast, the activation energies of DPL and DFL appear consistent with the energy requirement of a diffusion-controlled process, which requires less energy to transport reactants through the bulk fluid to the surface of the reacting particle.

This means both models can account for the dissolution kinetics of the leaching of silver from the WPCB in citric acid. While both models are capable of describing the dissolution kinetics, from the kinetic and Arrhenius modelling, it is evident that the DPL model offers a better fit and hence can relatively account for the dissolution kinetics better.

Table 8. *Kinetic parameters from the Arrhenius plots based on the SCMs for silver leaching in citric acid.*

Kinetic Parameters	Chemical Reaction	Diffusion through product layer	Diffusion through liquid film
Activation Energy, E_a (kJ/mol)	18.06	3.29	17.55
R^2	0.9932	0.9973	0.9936

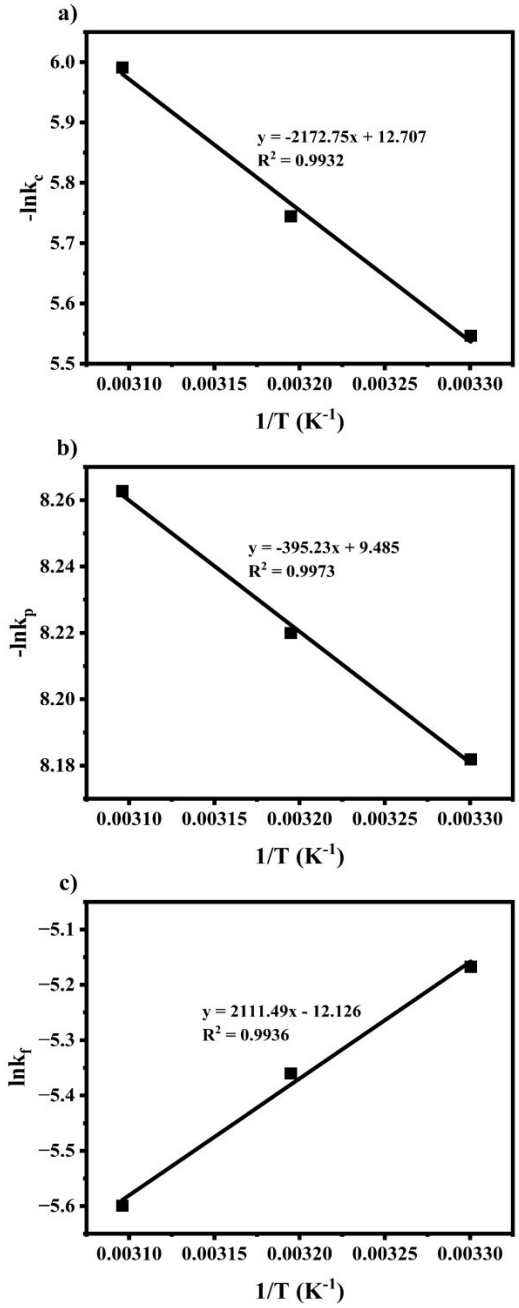


Fig. 12. Arrhenius plot for (a) Surface chemical reaction, (b) Diffusion through product layer, and (c) Diffusion through liquid models for the leaching of silver in citric acid

The empirical model for the description of the kinetic behaviour of the leaching reaction was derived using equations (11) and (13). The reaction order was determined to be 0.5072 from the plot of lnk_p versus lnC (Free, 2022; Dzikunu et al., 2024), and the pre-exponential factor, υ, was computed as 1.3 × 10^4 h^{-1} from the intercept of the DPL Arrhenius plot Figure 12b)). The comprehensive empirical kinetic model for the leaching of silver from WPCM in citric acid can then be expressed by Equation (24).

$$1 - \frac{2}{3}\alpha - (1-\alpha)^{\frac{2}{3}} = 1.3 \times 10^4 \times C^{0.5072} \times exp\left(-\frac{3.29\times10^3}{8.314T}\right) \times t \quad (24)$$

Conclusion

The present study was designed to investigate silver leaching from WPCBs using acetic and citric acids through a central composite design-response surface methodology (CCD-RSM) approach. The findings suggest that the quadratic model is suitable for predicting silver recovery from WPCBs. The quadratic model demonstrated reliable accuracy, statistically supported by high adjusted R^2 and low standard deviation values, with temperature, lixiviant concentration, and leaching time significantly influencing silver recovery outcomes. The coded second-order quadratic model equation highlighted the main factors affecting silver leaching, emphasizing the complex interactions of temperature (A), lixiviant concentration (B), and leaching time (C). The study found that temperature had a less pronounced effect in the acetic acid system compared to the citric acid system. Optimisation of the leaching process achieved silver recoveries of 11.48% at specific factor levels of 38.8°C, 2.5 M, and 4 hours for acetic acid, and 15.2% at 37.7 °C, 1 M, and 1.5 hours for citric acid, with desirability values nearing 1.0.

Subsequently, kinetic models were applied to study the leaching process dynamics, providing insight into the silver leaching kinetics. The model fit summary suggests that diffusion through the product layer mechanism best approximates the leaching kinetic behaviour, with R^2 > 0.85 across varying conditions. Investigations on the leaching kinetics temperature dependence were analysed using the Arrhenius plot, further validating that the reaction kinetics were principally controlled by diffusion through the product layer, with activation energies of 13.13 kJ/mol for acetic acid and 3.3 kJ/mol for citric acid.

Furthermore, this study enhances the precision of the leaching process, leading to a more efficient and sustainable method for recovering silver from WPCBs without the use of synthetic oxidants. The integration of RSM-CCD provided a comprehensive understanding of the critical interactions among process parameters that significantly impact silver recovery, paving the way for scalable, cost-effective WPCB management. The evidence presented in this work suggests that implementing the optimised parameters in industrial settings will yield a practical and economically viable approach for silver recovery. In the present research, the integration of kinetic frameworks with RSM-CCD provides a novel approach to analyse and optimise silver leaching, further improving predictability and control over the WPCB recovery process, and laying the foundation for future research in sustainable e-waste recycling.

Acknowledgment

The authors would like to appreciate the Organisation for Women in Science for Developing World (OWSD) Grant number 4500501094 for their financial support.

References

Arshadi, M., & Mousavi, S. M. (2014). Simultaneous recovery of Ni and Cu from computer-printed circuit boards using bioleaching: Statistical evaluation and optimisation. *Bioresource Technology*, *174*, 233–242. https://doi.org/10.1016/j.biortech.2014.09.140

Aydoğan, S., Motasim, M., & Ali, B. (2024). The novelty of silver extraction by leaching in acetic acid with hydrogen peroxide as an organic alternative lixiviant for cyanide. *Heliyon*, *10*(2), Article e24784 https://doi.org/10.1016/j.heliyon.2024.e24784

Barragan, J. A., Ponce De León, C., Alemán Castro, J. R., Peregrina-Lucano, A., Gómez-Zamudio, F., & Larios-Durán, E. R. (2020). Copper and Antimony Recovery from Electronic Waste by Hydrometallurgical and Electrochemical Techniques. *ACS Omega*, *5*(21), 12355–12363. https://doi.org/10.1021/acsomega.0c01100

Behera, S. K., Meena, H., Chakraborty, S., & Meikap, B. C. (2018). Application of response surface methodology (RSM) for optimisation of leaching parameters for ash reduction from low-grade coal. *International Journal of Mining Science and Technology*, *28*(4), 621–629. https://doi.org/10.1016/j.ijmst.2018.04.014

Birloaga, I., & Vegliò, F. (2016). Study of multi-step hydrometallurgical methods to extract the valuable content of gold, silver and copper from waste printed circuit boards. *Journal of Environmental Chemical Engineering*, *4*(1), 20–29. https://doi.org/10.1016/j.jece.2015.11.021

Cayumil, R., Khanna, R., Rajarao, R., Mukherjee, P. S., & Sahajwalla, V. (2016). Concentration of precious metals during their recovery from electronic waste. *Waste Management*, *57*, 121–130. https://doi.org/10.1016/j.wasman.2015.12.004

Click, N., Teknetzi, I., Tam, E. P. L., Tao, M., & Ebin, B. (2024). Innovative recycling of high purity silver from silicon solar cells by acid leaching and ultrasonication. *Solar Energy Materials and Solar Cells*, *270,* Article 112834. https://doi.org/10.1016/j.solmat.2024.112834

Clotilde Apua, M., & Madiba, M. S. (2021). Leaching kinetics and predictive models for elements extraction from copper oxide ore in sulphuric acid. *Journal of the Taiwan Institute of Chemical Engineers*, *121*, 313–320. https://doi.org/10.1016/j.jtice.2021.04.005

Cremona, A., & Mestl, G. (2023). Silver perspectives. *Chimica & Materiali*, *ANNO VII*(4), 46–52.

de Souza, W. B., Abreu, C. S., Rodrigues, G. D., Mageste, A. B., & de Lemos, L. R. (2018). Selective separation of Cu, Ni and Ag from printed circuit board waste using an environmentally safe technique. *Journal of Environmental Management*, *226*, 76–82. https://doi.org/10.1016/j.jenvman.2018.08.049

Dzikunu, P., Arthur, E. K., Gikunoo, E., Mensah-Darkwa, K., Akinwamide, S. O., & Vilaça, P. (2024). Optimisation of process parameters and kinetics of fluoride extraction from spent potlining using response surface methodology. *Journal of Environmental Management*, *367*, Article 121896. https://doi.org/10.1016/j.jenvman.2024.121896

Faraji, F., Alizadeh, A., Rashchi, F., & Mostoufi, N. (2022). Kinetics of leaching: A review. *Reviews in Chemical Engineering*, *38*(2), 113–148. https://doi.org/10.1515/revce-2019-0073

Forti, V., Balde, C. P., Kuehr, R., & Bel, G. (2020). *The Global E-waste Monitor 2020: Quantities, flows and the circular economy potential*. https://ewastemonitor.info/wp-content/uploads/2020/11/GEM_2020_def_july1_low.pdf

Free, M. L. (2022a). *Hydrometallurgy* (Second Ed.). https://doi.org/https://doi.org/10.1007/978-3-030-88087-3

Free, M. L. (2022b). *Rate Processes BT - Hydrometallurgy: Fundamentals and Applications* (M. L. Free (ed.); pp. 89–144). Springer International Publishing. https://doi.org/10.1007/978-3-030-88087-3_4

Golaghaei, F., Mohadesi, A., Ataei, S. A., Karimi, M. A., & Torabi, M. (2024). Optimising the leaching conditions of chalcopyrite/pyrite concentrate in Sarcheshmeh Copper Complex using response surface methodology. *Chemical Engineering Communications*, *211*(2), 221–228. https://doi.org/10.1080/00986445.2023.2230563

Habbache, N., Alane, N., Djerad, S., & Tifouti, L. (2009). Leaching of copper oxide with different acid solutions. *Chemical Leaching Journal, 152*, 503-508. https://doi.org/10.1016/j.cej.2009.05.020

Han, Y., Yi, X., Wang, R., Huang, J., Chen, M., Sun, Z., Sun, S., & Shu, J. (2020). Copper extraction from waste printed circuit boards by glycine. *Separation and Purification Technology*, *253*, Article 117463. https://doi.org/10.1016/j.seppur.2020.117463

Hao, J., Wang, X., Wang, Y., Wu, Y., & Guo, F. (2022). Optimising the Leaching Parameters and Studying the Kinetics of Copper Recovery from Waste Printed Circuit Boards. *ACS Omega*, *7*(4), 3689–3699. https://doi.org/10.1021/acsomega.1c06173

Hsu, E., Barmak, K., West, A. C., & Park, A.-H. A. (2019). Advancements in the treatment and processing of electronic waste with sustainability: a review of metal extraction and recovery technologies. *Green Chemistry*, *21*(5), 919–936. https://doi.org/10.1039/C8GC03688H

Ichikawa, S., Hirokawa, Y., Kurisaki, T., & Nakamura, T. (2023). Characterisation of a printed-circuit board by X-ray fluorescence and X-ray diffraction analyses for metal recovery. *Spectrochimica Acta - Part B Atomic Spectroscopy*, *210*, 1–7. https://doi.org/10.1016/j.sab.2023.106819

Jadhav, U., Su, C., & Hocheng, H. (2016a). Leaching of metals from large pieces of printed circuit boards using citric acid and hydrogen peroxide. *Environmental Science and Pollution Research*, *23*(23), 24384–24392. https://doi.org/10.1007/s11356-016-7695-9

Jadhav, U., Su, C., & Hocheng, H. (2016b). Leaching of metals from printed circuit board powder by an: Aspergillus Niger culture supernatant and hydrogen peroxide. *RSC Advances*, *6*(49), 43442–43452. https://doi.org/10.1039/c6ra04169h

Jansson, R. E. W. (1980). Electrochemical reaction engineering. In *Chemical Engineering Science,*. *35*(9), 1979-2004. https://doi.org/10.1016/0009-2509(80)80138-2

Khayyam Nekouei, R., Pahlevani, F., Golmohammadzadeh, R., Assefi, M., Rajarao, R., Chen, Y. H., & Sahajwalla, V. (2019). Recovery of heavy metals from waste printed circuit boards: statistical optimisation of leaching and residue characterisation. *Environmental Science and Pollution Research*, *26*(24), 24417–24429. https://doi.org/10.1007/s11356-019-05596-y

Khodaei, H., Fatmehsari Haghshenas, D., & Firoozi, S. (2022). Selective leaching of zinc from carbonate source using glycine as an ecofriendly lixiviant. *Minerals Engineering*, *185*, . https://doi.org/10.1016/j.mineng.2022.107680

Kumari, R., & Samadder, S. R. (2022). A critical review of the pre-processing and metals recovery methods from e-wastes. *Journal of Environmental Management*, *320*, Article 115887. https://doi.org/https://doi.org/10.1016/j.jenvman.2022.115887

Larba, R., Boukerche, I., Alane, N., Habbache, N., Djerad, S., & Tifouti, L. (2013). Citric acid as an alternative lixiviant for zinc oxide dissolution. *Hydrometallurgy*, *134–135*, 117–123. https://doi.org/10.1016/j.hydromet.2013.02.002

Levenspiel, O. (1998). *Chemical reaction engineering*. John Wiley & sons.

Li, L., Dunn, J. B., Zhang, X. X., Gaines, L., Chen, R. J., Wu, F., & Amine, K. (2013). Recovery of metals from spent lithium-ion batteries with organic acids as leaching reagents and environmental assessment. *Journal of Power Sources*, *233*, 180–189. https://doi.org/10.1016/j.jpowsour.2012.12.089

Li, L., Ge, J., Wu, F., Chen, R., Chen, S., & Wu, B. (2010). Recovery of cobalt and lithium from spent lithium ion batteries using organic citric acid as leachant. *Journal of Hazardous Materials*, *176*(1–3), 288–293. https://doi.org/10.1016/j.jhazmat.2009.11.026

Lisińska, M., Gajda, B., Saternus, M., Brozová, S., Wojtal, T., & Rzelewska-Piekut, M. (2022). The effect of organic acids as leaching agents for hydrometallurgical recovery of metals from PCBs . *Metalurgija*, *61*(3–4), 609–612.

Marinato, Y., Pavoski, G., Rosario, C. G. A., de Andrade, L. M., & Espinosa, D. C. R. (2023). Ag recovery from waste printed circuit boards of cell phone for synthesis of Ag nanoparticles and their antibacterial activity. *Journal of Material Cycles and Waste Management*, *25*(2), 970–984. https://doi.org/10.1007/s10163-022-01579-3

Mishra, G., Jha, R., Rao, M. D., Meshram, A., & Singh, K. K. (2021). Recovery of silver from waste printed circuit boards (WPCBs) through hydrometallurgical route: A review. *Environmental Challenges*, *4*. Article 100073. https://doi.org/10.1016/j.envc.2021.100073

Nan, T., Yang, J., Aromaa-Stubb, R., Zhu, Q., & Lundström, M. (2024). Process simulation and life cycle assessment of hydrometallurgical recycling routes of waste printed circuit boards. *Journal of Cleaner Production*, *435,* Artcle 140458. https://doi.org/10.1016/j.jclepro.2023.140458

Nekouei, R. K., Pahlevani, F., Rajarao, R., Golmohammadzadeh, R., & Sahajwalla, V. (2018). Two-step pre-processing enrichment of waste printed circuit boards: Mechanical milling and physical separation. *Journal of Cleaner Production*, *184*, 1113–1124. https://doi.org/10.1016/j.jclepro.2018.02.250

Onukwuli, O. D., & Nnanwube, I. A. (2022). Optimisation of zinc recovery from sphalerite using response surface methodology and particle swarm optimisation. *Periodica Polytechnica Chemical Engineering*, *66*(1), 20–29. https://doi.org/10.3311/PPch.17897

Petter, P. M. H., Veit, H. M., & Bernardes, A. M. (2015). Lixiviação de ouro e prata de placas de circuito impresso de celulares. *Revista Escola de Minas*, *68*(1), 61–68. https://doi.org/10.1590/0370-44672015680152

Preetam, A., Modak, A., Jadhao, P. R., Naik, S. N., Pant, K. K., & Kumar, V. (2022). A comprehensive study on the extraction of transition metals from waste random access memory using acetic acid as a chelating solvent. *Journal of Environmental Chemical Engineering*, *10*(6), Article 108761. https://doi.org/10.1016/j.jece.2022.108761

Raeisi, Z., Farajmand, B., Nakhostin Panahi, P., & Yaftian, M. R. (2023). Gold recovery from electronic wastes using a solvent extraction/selective back-extraction strategy. *Separation Science and Technology (Philadelphia)*, *58*(17–18), 2961–2970. https://doi.org/10.1080/01496395.2023.2260945

Saidan, M., Brown, B., & Valix, M. (2012). Leaching of electronic waste using biometabolised acids. *Chinese Journal of Chemical Engineering*, *20*(3), 530–534. https://doi.org/10.1016/S1004-9541(11)60215-2

Salahi, F., Zarei-Jelyani, F., Farsi, M., & Rahimpour, M. R. (2023). Optimisation of hydrogen production by steam methane reforming over Y-promoted Ni/Al2O3 catalyst using response surface methodology. *Journal of the Energy Institute*, *108*, Article 101208. https://doi.org/10.1016/j.joei.2023.101208

Suanon, F., Sun, Q., Dimon, B., Mama, D., & Yu, C. P. (2016). Heavy metal removal from sludge with organic chelators: Comparative study of N, N-bis(carboxymethyl) glutamic acid and citric acid. *Journal of Environmental Management*, *166*, 341–347. https://doi.org/10.1016/j.jenvman.2015.10.035

Syed, S. (2016). Silver recovery aqueous techniques from diverse sources: Hydrometallurgy in recycling. *Waste Management*, *50*, 234–256. https://doi.org/10.1016/j.wasman.2016.02.006

Tanaydin, M. K., Tanaydin, Z. B., & Demirkiran, N. (2022). Optimisation of process parameters and kinetic modelling for leaching of copper from oxidized copper ore in nitric acid solutions. *Transactions of Nonferrous Metals Society of China (English Edition)*, *32*(4), 1301–1313. https://doi.org/10.1016/S1003-6326(22)65875-8

Wang, F., Zhao, Y., Zhang, T., Duan, C., & Wang, L. (2015). Mineralogical analysis of dust collected from typical recycling line of waste printed circuit boards. *Waste Management*, *43*, 434–441. https://doi.org/10.1016/j.wasman.2015.06.021

Wu, D., Wen, S., & Deng, J. (2015). Leaching kinetics of cerussite using a new complexation reaction reagent. *New Journal of Chemistry*, *39*(3), 1922–1929. https://pubs.rsc.org/en/content/articlelanding/2015/nj/c4nj01549e

Yin, J., Li, G., He, W., Huang, J., & Xu, M. (2011). Hydrothermal decomposition of brominated epoxy resin in waste printed circuit boards. *Journal of Analytical and Applied Pyrolysis*, *92*(1), 131–136. https://doi.org/10.1016/j.jaap.2011.05.005

Yoğurtcuoğlu, E. (2023). Multi-metal recovery from flotation tailings with citric acid on the NACI media. *Journal of Scientific Reports-A*, *053*, 59–73. https://doi.org/10.59313/jsr-a.1243469

Zan, N. N. M., Lotfi, W. N. A. W. M., & Yusof, Y. M. (2024). Thermodynamic Study of Silver-Citrate-Hydrogen Peroxide System for the Extraction of Silver From Electronic Waste. *Journal of Engineering Science and Technology*, *19*(1), 146–162. https://jestec.taylors.edu.my/Vol%2019%20Issue%201%20February%20%202024/19_1_11.pdf

Zhang, H., Yu, H., Sun, W., Lin, S., & Zhang, C. (2024). Beneficiation of silver and silver-bearing lead–zinc ores: A review. *Minerals Engineering*, *208, Article 108168.* https://doi.org/10.1016/j.mineng.2024.108608

Zhu, X. nan, Ni, Y., Wang, D. zhang, Zhang, T., Qu, S. juan, Qiao, F. ming, Ren, Y. guang, Nie, C. chen, Lyu, X. jun, Qiu, J., & Li, L. (2020). Effect of dissociation size on flotation behavior of waste printed circuit boards. *Journal of Cleaner Production*, *265.* Article 121840. https://doi.org/10.1016/j.jclepro.2020.121840